Journal of Electroanalytical Chemistry 628 (2009) 35–42

Contents lists available at ScienceDirect

Journal of Electroanalytical Chemistry

journal homepage: www.elsevier.com/locate/jelechem

Scanning electrochemical microscopy of HeLa cells – Effects of ferrocene methanol and silver ion

Xiao Li, Allen J. Bard *

Department of Chemistry and Biochemistry, University of Texas at Austin, 1 University Station A5300, Austin, TX 78712-0165, USA

ARTICLE INFO

Article history:
Received 17 September 2008
Received in revised form 19 December 2008
Accepted 5 January 2009
Available online 12 January 2009

Keywords:
SECM
HeLa
Silver ion

ABSTRACT

The viability and activity of HeLa cells were probed using scanning electrochemical microscopy (SECM). The feedback generated by HeLa cells during scanning depends on the electrochemical mediator. Living HeLa cells generated positive feedback when ferrocene methanol (FcMeOH) was oxidized at the tip, showing that the cells reduced $FcMeOH^+$. The positive feedback with FcMeOH changed to negative feedback when the HeLa cells were exposed to toxic treatments, i.e. CN^- or UVC radiation, suggesting that $FcMeOH^+$ reduction can be used to monitor cell activity. Living HeLa cells also accumulate FcMeOH after exposure times of a few h, but the presence of mM concentrations of FcMeOH has no apparent effect on the cell viability. The effect of Ag^+ (known to be toxic to bacteria at the 10 μM level) on HeLa cells was probed using the FcMeOH as an indicator. The activity of the HeLa cells was not affected in a culture medium containing Ag^+ up to 10 mM. The uptake of Ag^+ by living and dead HeLa cells was small and nearly the same, indicating that even at high Ag^+ concentrations in the culture medium, only a small amount of Ag^+ is accumulated within the cells.

1. Introduction

Because the activity of living cells is sensitive to the environment and external chemical and physical stimuli, it is useful to be able to monitor the cell activity in real time, for example in drug screening. A number of scanning probes have been used for biological imaging, such as atomic force microscopy [1], near field scanning optical microscopy [2] and confocal laser scanning microscopy [3,4]. Scanning electrochemical microscopy (SECM) has the advantage that it can chemically image systems such as biological systems with μm or sub-μm resolution [5–7]. Images of the reduction–oxidation processes can provide information about cell morphology, enzymatic activity and cellular functions (e.g., metabolism) [8–10].

SECM has been applied in characterizing the activity of various cells. The metabolic activity of *Escherichia coli* cells embedded in collagen gel microstructures was investigated based on the O_2 consumption rate and the reduction of $Fe(CN)_6^{3-}$ [11]. Oxygen evolution above a single stomate was monitored in vivo to study guard cells and Cd-induced plant stress [12,13]. The spatial distribution of the respiratory activity in neuronal cells [14] was also examined, as well as the contrast between normal and metastatic human breast cells [15]. Furthermore, SECM has also been used for cytological diagnosis and for evaluating the cytotoxic effects of chemicals [16]. The effects of anticancer drugs were examined based on the respiratory activity of a multicellular spheroid [17]. Recently, constant-distance mode scanning was employed to image small changes in neuron cell morphology [18] and to detect amperometrically the release of adrenaline and noradrenaline out of single secretory vesicles upon stimulation [19,20].

Oxygen reduction at the tip has frequently been employed in SECM studies of living cells, because oxygen concentration can be directly related to the respiratory activity of the cells. The feedback effect of other mediators, like menadione, was also examined on cells during SECM scanning [8,21]. In such studies negative feedback is often obtained with hydrophilic mediators, like ferrocene carboxylate, that cannot cross the cell membrane, while positive feedback is generated with hydrophobic ones.

Various silver preparations have been of interest because of their antibacterial effects. For example, μM concentrations of Ag^+ have been reported to be lethal to both Gram-positive and Gram-negative bacteria [22,23]. Although the exact mode of action is still unknown, silver may uncouple the respiratory chain from oxidative phosphorylation [24,25], bind to membrane-bound enzymes and proteins containing thiol groups [26], and interact with intracellular components in cytoplasm [27]. Investigation of the effect of chloride on the growth inhibition of algae suggests that silver toxicity is a direct result of intracellular accumulation rather than cell surface interactions [28]. In addition, active Ag^+ efflux was reported for silver-resistant *E. coli* and was attributed by genetic studies to the transmembrane CusCFBA protein complex [29,30].

* Corresponding author. Tel.: +1 512 471 3761; fax: +1 512 471 0088.
E-mail address: ajbard@mail.utexas.edu (A.J. Bard).

0022-0728/$ - see front matter © 2009 Elsevier B.V. All rights reserved.
doi:10.1016/j.jelechem.2009.01.002

Recent electrochemical studies on *E. coli* confirmed the Ag^+ effect on the respiratory chain and suggested that 60% of Ag^+ taken up is transported into the cell while 40% binds to the outer membrane [31]. Electrochemical methods are valuable tools for probing the mechanism of silver toxicity and antimicrobial action.

Antimicrobial agents like Ag^+ should not only exhibit maximum toxicity and inhibition of bacterial growth, as already have been extensively investigated, but also show minimum cytotoxicity on mammalian tissue. The effects of various metal ions on mammalian fibroblasts and human tissue mast cells have been tested in vitro [32–34]. Metal cations produce dose-dependent cytopathogenic effects in distinct cell types. With short exposure, the rate of cation uptake correlates with depression of succinic dehydrogenase activity, while protein synthesis is depressed with longer exposure. Silver ions inhibit the proliferation of human dermal fibroblasts after 24 h exposure mainly through the inhibitory action on DNA synthesis and depletion of intercellular ATP content [35]. Further investigation of the Ag^+ effect on the cell activity using electrochemical methods can aid our understanding of the mechanism of silver action on cells.

In this paper, several mediators were first tested on HeLa cells and the relationship between the feedback of FcMeOH and the viability of the HeLa cell was then determined. The effect of Ag^+ on the activity of HeLa cells was tested by using FcMeOH oxidation as an indicator of cell viability and the uptake of Ag^+ by the HeLa cells was also measured.

2. Experimental

2.1. Chemicals

All chemicals were reagent grade and used as received. All solutions were prepared with deionized water (Milli-Q, Millipore Corp.). D-Glucose, $AgNO_3$ and FcMeOH ($C_{11}H_{12}FeO$) were obtained from Aldrich (St. Louis, USA); KCN, $MgSO_4$, K_2SO_4 and $K_3Fe(CN)_6$ were obtained from Fisher (Pittsburgh, USA); K_2HPO_4 and KH_2PO_4 were purchased from J.T. Baker (Phillipsburg, USA); $Co(bpy)_3Cl_2$, $Co(phen)_3Cl_2$, $K_4Fe(CN)_6$ and TMPD were purchased from Sigma (St. Louis, USA).

2.2. Cell culture

The HeLa cells (human cervical cancer cells) were a generous gift from Dr. Lara K. Mahal (University of Texas at Austin). Cells were grown and maintained in Dulbecco's modified Eagle's medium/10% heat-inactivated fetal bovine serum while adhering to the bottom of the Petri dish. The temperature was maintained at 37.5 °C in a water-jacketed incubator (model 2310, VWR Scientific) with 5% CO_2. HeLa cells with coverage of 60–90% were used for the experiments. Since Ag^+ was tested in the experiments, the Cl^--containing growth medium was not used in electrochemical measurements. Thus, before experiments, the growth medium was removed, the dish was rinsed several times, and 2 mL of experimental culture medium (10 mM HEPES, 10 mM glucose, 75 mM Na_2SO_4, 1 mM $MgSO_4$ and 3 mM K_2SO_4) was added into the Petri dish. The viability of HeLa cells in this culture medium was tested by Trypan Blue and the cells remained alive for at least 1 day at room temperature in air.

2.3. Irradiation

HeLa cells were irradiated as a monolayer in a 35 mm Petri dish without the dish cover, as polystyrene has significant absorption in the UV region. During the irradiation, the HeLa cells were immersed in 2 mL experimental culture medium containing 1 mM FcMeOH. UV radiation generated by a photochemical reactor (mercury lamp) (RPR-100, Rayonet, Hamden, CN) was used, where 80% of the incident radiation is centered at 253.7 nm. The irradiance at the culture medium surface was measured to be ~0.045 W/m^2 in the UVC region.

2.4. SECM experiments

Ultramicroelectrodes (UMEs) (Pt, radius, a = 10 μm, relative radius of insulator, r_{ins}, is given by RG = r_{ins}/a of 5 were used in the experiments. A detailed description of their fabrication and characterization has been reported elsewhere [36]. A Hg modified Pt electrode (10 μm) (Hg/Pt) was used in some experiments for its better reproducibility and stability in measurements of O_2 reduction. A Hg drop was deposited on the Pt electrode by holding the potential at 0.04 V for 200 s in a deoxygenated solution containing 1 M KNO_3, 0.5% HNO_3 and 5.7 mM $Hg_2(NO_3)_2$. The resulting Hg drop had a semispherical shape with a diameter of ca. 15 μm [37]. Pt wire (0.5 mM diameter; Goodfellow, Cambridge, UK) was used as the counter electrode. An Hg/Hg_2SO_4 electrode (Radiometer, Copenhagen) was used as the reference electrode. All potentials reported in this paper are referenced to NHE. The SECM (model 900, CH Instruments, Austin, TX) was used to obtain the electrochemical results.

For SECM imaging experiments, a Petri dish with cells adhering to the bottom was directly used as a part of the electrochemical cell. To obtain better images and have more active cells, all experiments were carried out before the cells reached 100% confluency. After the culture medium was changed, the tip was moved in the z direction (perpendicular to the dish bottom) by using either FcMeOH oxidation (E = 0.6 V) in a solution containing 1 mM FcMeOH, or O_2 reduction (E = −0.3 V) in a solution without FcMeOH. All images were obtained while the tip was 15–20 μm above the dish bottom. If the tip was farther, both the contrast and the resolution of the cell images were lower. If the tip was too close, there was risk that the tip might scratch or even remove cells, as HeLa cells have a height of around 8–10 μm. Once the tip was positioned in the z direction, it was scanned using the piezoelectric drive in the x–y plane over a region with moderate cell coverage, while the tip potential was held where the desired reaction occurred. The tip was scanned from the upper-left corner, to the lower-right corner of the image, with a recording time per image of 3 ~ 10 min, depending on the image size and the tip scan rate. All experiments were carried out in air without de-aeration.

The same cells in a Petri dish were examined repeatedly in different culture media. When changing the solution, the electrode tip was first withdrawn in the z direction out of the solution. Then, the solution was changed and the dish was rinsed three times using a pipette. Since the Petri dish was stabilized on the sample stage using double sided tape, little effect was observed on the position of the Petri dish during the process. Finally, the tip was lowered and its position in z direction was determined by the approach curve.

2.5. Ag^+ effect on cells

A SECM image of HeLa cells with 80% cell coverage was first obtained in a culture medium containing 1 mM FcMeOH. Then, the electrode was withdrawn 5 mM in the z direction, to a point above the solution. Without splashing the solution onto the tip, the culture medium of the HeLa cells was changed to one containing 10 mM $AgNO_3$. After 1 h, the Ag^+-containing solution was taken out. After rinsing several times, fresh culture medium containing 1 mM FcMeOH was added for SECM experiments.

Ag^+ accumulation by dead and living HeLa cells was studied using an anodic stripping voltammetry technique [38]. A Pt UME

(radius of 12.5 μm) was used. The potential was first scanned from 0.44 V to 0.84 V at 0.1 V/s, then held at 0.84 V for 30 s to remove any trace Ag from the electrode surface, followed by a second sweep from 0.44 to 0.84 V at 0.1 V/s. After holding at 0.34 V for 1 s to accumulate Ag on the surface, the potential was swept for a third time. The stripping current of Ag at ca. 0.7 V during the third sweep was used to indicate the Ag^+ concentration in the solution. This stripping technique was ended by holding the tip potential at 0.84 V for 20 s to ensure the clearance of Ag off the electrode. The UME was occasionally mechanically polished to generate a new surface for reproducible results. Some deactivation of the Pt surface towards Ag^+ deposition and stripping with time was found. Highly confluent HeLa cells were used with coverage of 90%. Since dead cells that detach from the Petri dish tend to contaminate the Pt surface, formaldehyde treatment (4% solution for 15 min at room temperature) was used to ensure that the dead HeLa cells still adhered to the dish bottom.

3. Results

3.1. Cell activity monitored by oxygen reduction

SECM has previously been used to monitor the metabolic activity of mammalian cells at the single cell level [5], where O_2 reduction current was measured to indicate the respiration of living cells [39]. To test this, HeLa cells were first imaged using the O_2 reduction. The images were obtained (Fig. 1A) at −0.3 V for O_2 reduction and (Fig. 1B) at 0.6 V for FcMeOH oxidation. The Pt UME was held 18 μm above the dish bottom scanned at 3 μm/s. For comparison, the same group of HeLa cells was scanned at both potentials. In all SECM images, a yellow color indicates higher current while green shows a lower current.[1]

When O_2 reduction occurs on the tip, the current above the HeLa cells is smaller than that of the background signal away from HeLa cells, as indicated by the green color in Fig. 1A. This negative feedback has been observed in previous studies and is attributed to the lower concentration of O_2 near cells due to their O_2 uptake and respiration activities (a shielding effect), as well as the blocking effect the cells have on O_2 diffusion [40]. Although O_2 reduction has been used to monitor the viability of living cells, it has the drawback that the Pt electrode surface that catalyzes this reduction tends to change with time, even in the absence of cells [41]. Shown in Fig. 1A, as the background color changes from yellow at the top left to light yellow at the bottom right of the image, a 45% decrease of the current was observed. The instability of O_2 reduction causes difficulty in obtaining clear and reproducible images of cells [41]. The slightly lighter spots above the right part of the cells in the image may be due to the fast oxygen transport across the cell membrane [8].

3.2. Cell activity monitored by FcMeOH oxidation

In Fig. 1B, when FcMeOH oxidation occurs on the tip, the HeLa cells are yellow, while the background color away from HeLa cells is green. This indicates that the current from FcMeOH oxidation is higher when the tip is directly above a HeLa cell than when the tip is over the bare dish. This positive feedback suggests that the HeLa cell below the tip can participate in the FcMeOH–$FcMeOH^+$ redox cycle [42] in the gap between the tip and the cell. In other words, the HeLa cell can reduce $FcMeOH^+$ generated by the tip. The FcMeOH diffuses back to the tip, leading to an increase in the oxidation current. Compared with O_2 reduction, the oxidation of FcMeOH on a Pt electrode was more stable, so that clear and reproducible images of cells can be easily obtained.

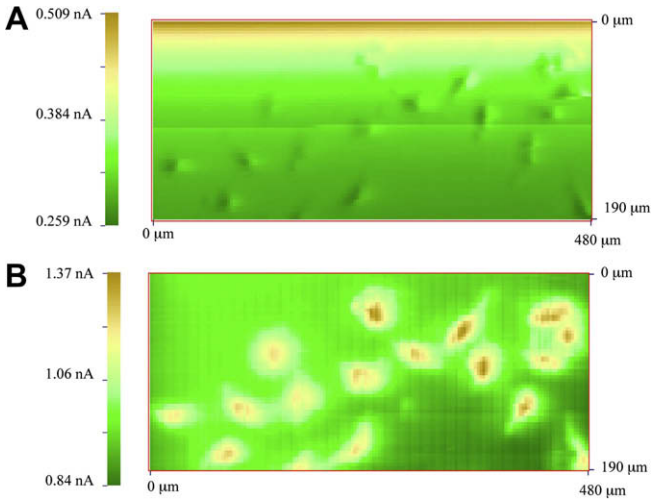

Fig. 1. The SECM images of HeLa cells in a culture medium containing 1 mM FcMeOH. A 10 μm Pt UME was scanned 18 μm above the dish bottom at 3 μm/s. The electrode potential was held at (A) −0.3 V for the O_2 reduction reaction and (B) 0.6 V for the FcMeOH oxidation reaction.

3.3. Cell viability test using O_2 reduction and FcMeOH oxidation upon exposure to CN^-

Fig. 2A shows two SECM images of one HeLa cell with the same scale at 3 min and 50 min following the addition of 30 mM KCN to the culture medium. The Hg/Pt electrode was held at −0.6 V and the O_2 reduction current was measured. Right after the addition of CN^-, the left image shows a dark green spot corresponding to the location of a living HeLa cell on the dish. After 50 min, the green color corresponding to the cell becomes light, which indicates a higher O_2 reduction current when the tip is right above the dead HeLa cell.

Fig. 2B shows the SECM images of two HeLa cells at 0 min and 32 min following the addition of 30 mM KCN to a culture medium containing 1 mM FcMeOH. The Pt UME was held at 0.6 V and FcMeOH oxidation occurred on the tip. Before the addition of CN^-, the SECM image showed two yellow spots corresponding to the location of two living HeLa cells on the dish. However, 22 min after the CN^- addition, negative feedback was observed with a smaller FcMeOH oxidation current when the tip was above the HeLa cells, indicated by the green color.

Fig. 2C schematically shows the relative geometry for the dish current I_d and cell current, I_c. The dish current, I_d, was the current when the tip was near a HeLa cell but directly over the bare Petri dish, while the cell current, I_c, was the current when the tip was directly above the HeLa cell. Both I_d and I_c have positive values. Fig. 2D shows the time-dependent variation of the feedback currents, calculated as $(I_c - I_d)$, measured by SECM following the addition of 30 mM KCN. The black and red dots are the feedback currents of O_2 reduction and FcMeOH oxidation, respectively. During the first 15 min, HeLa cells generated negative feedback for O_2 reduction and positive feedback for FcMeOH oxidation. At about 18 min, the positive feedback currents of FcMeOH oxidation decreased to negative feedback values. After about 20 min, the negative feedback currents for O_2 reduction increased to a smaller negative value. The small negative feedback currents observed 25 min after the addition of CN^- are due to the blocking effect that the cells have on either FcMeOH or O_2 diffusion and indicate the cessation of HeLa cell activity. The time needed for the rapid

[1] For interpretation of color in Figs. 1–7, the reader is referred to the web version of this article.

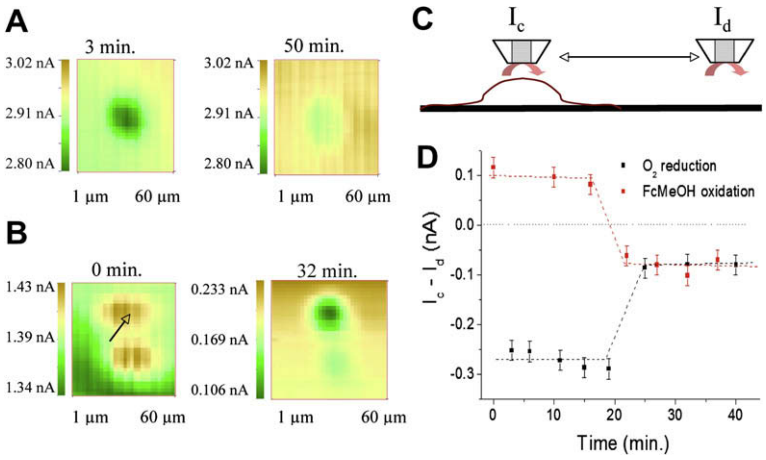

Fig. 2. SECM images of HeLa cells following the addition of 30 mM KCN into a culture medium (A) without, and (B) with 1 mM FcMeOH. (A) A Hg/Pt UME at −0.6 V and (B) a Pt UME at 0.6 V was scanned 15 μm above the dish bottom at 3 μm/s. All images are 60μm × 70 μm. (C) A schematic graph for the dish current, I_d, and the cell current, I_c. The brown line outlines the shape of a HeLa cell on the Petri dish. The red curved arrow indicates the reaction occurring on the electrode. (D) Variation of the feedback currents measured by SECM with time. Feedback currents were calculated as the difference between I_d and I_c. Error bars are from two experiments. The dashed lines are guides for the eye.

decrease of the activity of HeLa cells was about 20 min, which matches well with previously reported results [41].

Cyanide ion is known to be lethal for mammalian and bacterial cells [41,43]. Cyanide may bind tightly to cytochrome oxidase and block electron transport in the respiration chain. These experiments clearly suggest that both the O_2 reduction and FcMeOH oxidation reaction can be used to monitor the cell activity on the Petri dish. The positive feedback of FcMeOH is due to the interaction of $FcMeOH^+$ with living HeLa cells. Dead cells only show negative feedback.

3.4. Cell viability test using FcMeOH oxidation upon UVC radiation

The relationship between cell viability and FcMeOH feedback was further tested by exposing HeLa cells to UVC radiation. Before the irradiation, all HeLa cells generated positive feedback for the FcMeOH oxidation. Fig. 3A shows a SECM image of HeLa cells in a culture medium containing 1 mM FcMeOH after a dose of 16 J m^{-2} of UVC radiation. After the irradiation, most of the HeLa cells showed negative feedback. The irregular stretched shape of some cells in the lower part of the image is caused by tip contact leading to dragging of some cells by the scanning electrode tip. Since dead HeLa cells do not adhere strongly to the dish, the moving tip can remove loose cells from the surface, especially if a cell attaches to the tip end.

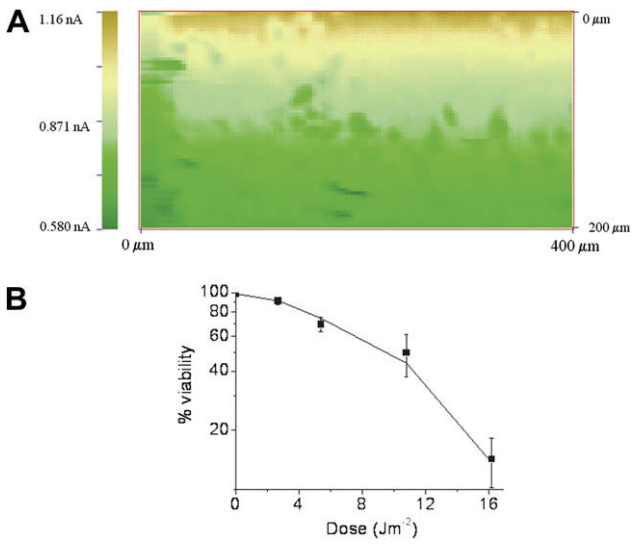

Fig. 3. (A) SECM images of HeLa cells obtained in a culture medium containing 1 mM FcMeOH after a 16 Jm^{-2} dose of UVC radiation. A 10 μm Pt UME at the potential of 0.6 V was scanned at 3 μm/s. All images are 400 μm × 200 μm. (B) The effect of UVC radiation on the viability of the HeLa cells. The error bar was determined from different experiments. The line is a guide for the eye.

Fig. 3B shows the dependence of cell viability on the dose of UV radiation. Cell viability was calculated from the ratio between the number of HeLa cells generating positive feedback and the total cell number within the area. Indicated by the solid line, exposure to UVC radiation results in a dramatic decrease in HeLa cell viability. After a dose of 16 J m^{-2}, only 15% of the HeLa cells generated positive feedback for FcMeOH oxidation. Similar effects of UVC radiation on the survival rate of HeLa cells was reported previously [44]. Exposure of mammalian cells to UV radiation is known to damage the cellular DNA, leading to either cell mutation or death [45,46].

Both CN^- and UV experiments suggest that dead HeLa cells generate negative feedback while living cells generate positive feedback. Hence, the FcMeOH oxidation reaction can be used as an electrochemical indicator to test the viability of HeLa cells.

3.5. Glucose effect on the positive feedback of FcMeOH

The species within the HeLa cells that can reduce $FcMeOH^+$ are of interest in understanding the FcMeOH feedback. As one of the most important nutritional reductants for mammalian cells, the effect of glucose on the feedback behavior of HeLa cells was tested. Fig. 4A shows SECM images of HeLa cells in a culture medium containing 1 mM FcMeOH without glucose. Then, the electrode was positioned and held 8 μm above the top of a HeLa cell at 0.6 V, indicated by the arrow in Fig. 4A. One hour later, image Fig. 4B was obtained.

Positive feedback of FcMeOH was still observed even after 1 h consumption of reducing equivalents within the single HeLa cell. The total amount of charge consumed during the 1 h experiment can be calculated to be 4.3 μC through integration of the current–time curve. If only 10% of the tip current due to the oxidation of FcMeOH was regenerated by the HeLa cell directly below it, the cell would have donated electrons to the $FcMeOH^+$ in an amount equivalent to q = 0.43 μC. Since there was no glucose in the culture medium, the HeLa cell could not obtain extra glucose from the

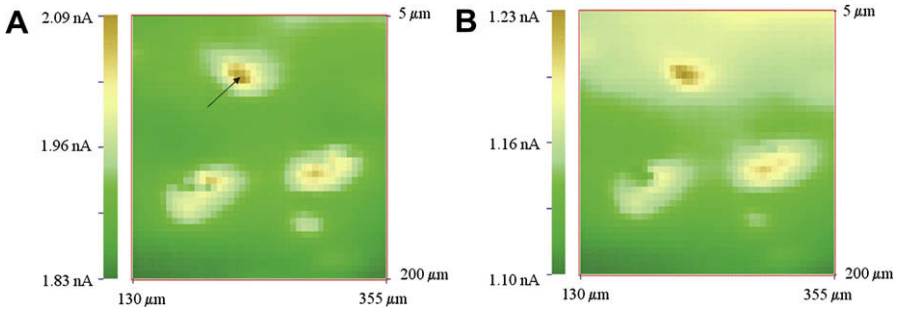

Fig. 4. SECM images of HeLa cells monitored by the FcMeOH oxidation reaction in a culture medium without glucose, but containing 1 mM FcMeOH. A 10 μm Pt electrode at the potential of 0.6 V was scanned at 5 μm/s. Images were taken (A) before, and (B) after the potential step at 0.6 V for 1 h, while the electrode was held 8 μm above the HeLa cell indicated by the black arrow in (A).

solution. With the assumption that all glucose undergoes complete oxidation, the maximum charge, q_g, generated only from glucose within a single cell can be calculated from Eq. (1) to be approximately 26 nC,

$$q_g = nFC_gV_c = \frac{4}{3}nFC_g\pi r_c^3 \quad (1)$$

where $n = 6$ is the total number of electrons for glucose oxidation, F is the Faraday constant, V_C is the volume of one HeLa cell, $r_c \sim 13$ μm is the average radius of a HeLa cell in suspension, and C_g is the concentration of glucose within the cell, taken to be ~5 mM [47]. The q is more than 10 times q_g, suggesting additional sources of electrons that produce the observed positive feedback such as glutamine and NADH [48,49].

3.6. Feedback of different electrochemical mediators: $Co(bpy)_3^{2+}$, $Co(phen)_3^{2+}$, $Fe(CN)_6^{4-}$, TMPD and FcMeOH

Fig. 5A–F shows SECM images of HeLa cells obtained using a 10 μm Pt UME in a culture medium containing 1 mM of either $Co(bpy)_3^{2+}$, $Co(phen)_3^{2+}$, $Fe(CN)_6^{4-}$, TMPD or FcMeOH, respectively. All images were taken of the same group of HeLa cells while the tip potential was held for the appropriate oxidation reaction.

In Fig. 5A–C the oxidation current of the mediator above a HeLa cell was lower than that when the tip was away from the cells. This negative feedback observed for $Co(bpy)_3^{2+}$, $Co(phen)_3^{2+}$ and $Fe(CN)_6^{4-}$ was due to the blocking effect by the cell of the mediator diffusion as explained above. The same type of negative feedback was also observed previously with other hydrophilic mediators, such as $Ru(NH_3)_6^{2+}$ and $Ru(CN)_6^{4-}$ on human breast cancer cells [8].

Fig. 5D and E were both taken in a culture medium containing 1 mM TMPD, while the tip potential was held at potentials for the first and second oxidation of TMPD, respectively. Both images exhibit positive feedback, which indicates reduction of $TMPD^+$ and $TMPD^{2+}$ by the cells below the tip. Interestingly, the oxidation current in Fig. 5E is twice that in Fig. 5D, which agrees well with the number of electrons transferred. For comparison, the SECM image obtained in a solution containing 1 mM FcMeOH is shown in Fig. 5F. Similar behavior of HeLa cells has been reported previously with other redox species [8,15].

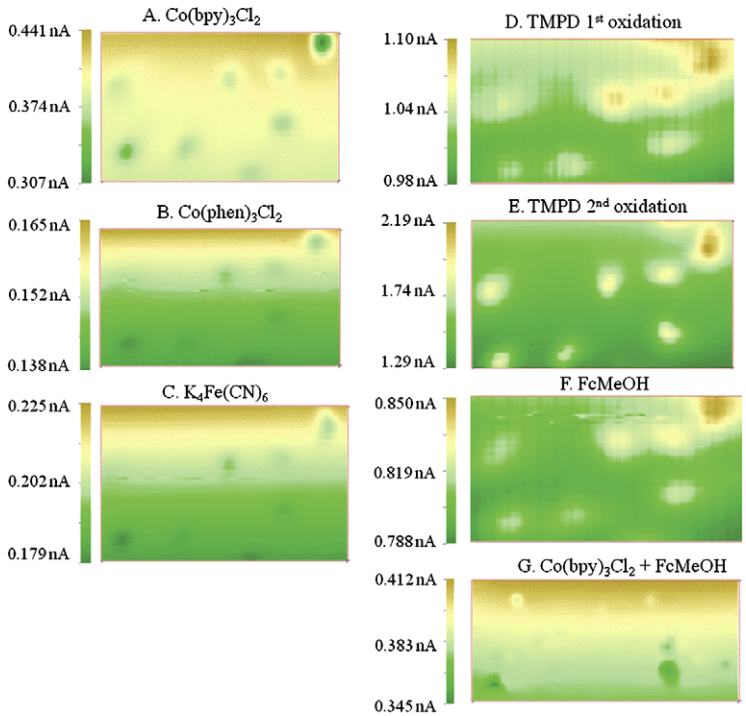

Fig. 5. SECM images of HeLa cells in a culture medium containing different mediators. A 10 μm Pt UME was scanned 20 μm above the dish bottom at 2 μm/s. Oxidation of the mediator occurred on the tip during scanning: (A) 1 mM $Co(bpy)_3Cl_2$ at E (tip potential) = 0.6 V; (B) 1 mM $Co(phen)_3Cl_2$ at E = 0.6 V; (C) 1 mM $K_4Fe(CN)_6$ at E = 0.6 V; (D) 1 mM TMPD at E = 0.5 V for first oxidation; (E) 1 mM TMPD at E = 0.9 V for second oxidation; (F) 1 mM FcMeOH at E = 0.6 V and (G) 1 mM Co(bpy)3Cl2 + 0.01 mM FcMeOH at E = 0.6 V. The SECM images A–F are 200 μm × 130 μm, and G is 280 μm × 130 μm.

The two oxidation potentials of TMPD cover a wider range, from 0.27 to 0.75 V, than those of the other mediators tested here. The different feedback behavior observed for these mediators strongly suggests that the equilibrium potential of the mediators may be important, but is not the only factor responsible for the observation of positive feedback. The charge on every mediator that showed negative feedback is greater than 1, leading to higher hydrophilicity. The high charges and low solubility of these mediators in the lipid bilayer suggest that the membrane of the HeLa cells is impermeable to these mediators. Thus, these mediators can only interact with HeLa cells by reacting at the cell surface, not within the membrane. Furthermore, if the HeLa cell contained an electron carrier M/M^+ within the membrane, the reduction of oxidant A^+ by the HeLa cell would be highly dependent upon its reduction potential. Since the equilibrium potentials of $Co(bpy)_3^{3+}$, $Co(phen)_3^{3+}$ and $Fe(CN)_6^{3-}$ are more positive than that of TMPD, these mediators are more easily reduced than $TMPD^+$. Thus, the observed positive feedback for TMPD and negative feedback for the other three mediators suggests that no naturally contained M/M^+ in the membrane of the HeLa cells can work as the electron carrier.

Another question about this mechanism is whether FcMeOH/$FcMeOH^+$ can act as the M/M^+ couple in the plasma membrane of the HeLa cells. The following experiments were thus performed. An image of HeLa cells were first obtained in a culture medium containing 0.01 mM FcMeOH and positive feedback was observed (data not shown). Then, 1 mM $Co(bpy)_3^{2+}$ was added to the solution and SECM images were obtained, shown in Fig. 5G. Although positive feedback was observed with 0.01 mM FcMeOH, negative feedback was observed for HeLa cells with the addition of 1 mM $Co(bpy)_3^{2+}$, just as it was in solution without FcMeOH in Fig. 5A. This negative feedback strongly suggests that FcMeOH/$FcMeOH^+$ cannot act as an electron carrier within the plasma membrane and the proposed mechanism does not work. Hence, the interaction between FcMeOH and HeLa cells most likely occurs with the diffusion of FcMeOH through the membrane and into the cytoplasm. Experiments showing FcMeOH accumulation within HeLa cells and its subsequent leakage out, with simulation of the behavior and estimates of the rates of the processes, will be described elsewhere.

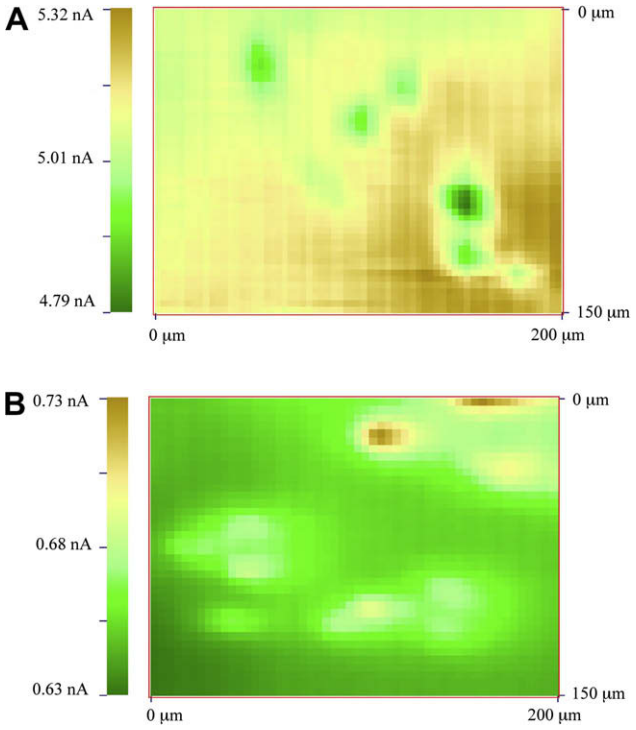

Fig. 6. SECM images of HeLa cells after 1 h incubation in a culture medium containing 10 mM Ag^+. (A) The Hg/Pt UME was held at −0.6 V. (B) The Pt UME was held at 0.6 V in a culture medium containing 1 mM FcMeOH. The electrode was scanned 15 μm above the dish bottom at 3 μm/s.

4. Effect of Ag^+ on HeLa cells

4.1. Cell activity monitored by O_2 reduction and FcMeOH oxidation upon exposure to Ag^+

Fig. 6 shows SECM images of HeLa cells after the 1 h treatment of Ag^+ in a culture medium (Fig. 6A) without, and (6B) with 1 mM FcMeOH. Both O_2 reduction and FcMeOH oxidation were used to monitor HeLa cell viability and the resulting images are shown in Fig. 6A and B, respectively. As discussed above, the strong negative feedback observed for O_2 reduction and positive feedback observed for FcMeOH oxidation is generated only from living HeLa cells. Thus, the higher current on HeLa cells in Fig. 6 demonstrates that the HeLa cells are still active after a 1 h exposure to 10 mM Ag^+. Similar results were obtained with lower Ag^+ concentrations (range from 10 μm to 1 mM). HeLa cells can either prevent Ag^+ from leaking across the plasma membrane, or deactivate Ag^+ before it interferes with the respiratory chain, as it does with *E. coli*. To investigate the interaction between HeLa cells and Ag^+, the consumption of Ag^+ within HeLa cells was studied.

4.2. Ag^+ Consumption of HeLa cells

Fig. 7 shows the time dependence of the relative Ag^+ concentration in solution determined by anodic stripping analysis for living (red circles) and dead (black squares) HeLa cells. At $t = 0$ min, the culture medium was changed to one containing 0.5 mM Ag^+. The Petri dish was occasionally shaken slightly to ensure homogenous distribution of Ag^+ in the solution. Both the dead and living HeLa cells caused a decrease in the Ag^+ concentration in solution. The concentration of Ag^+ in solution dropped rapidly within the first 15 min, which indicates fast adsorption or uptake of Ag^+ by the cells. Then, the concentration gradually reached a plateau after 20 min, indicating equilibrium between the cells and Ag^+ in solution. Control experiments in the absence of cells showed no de-

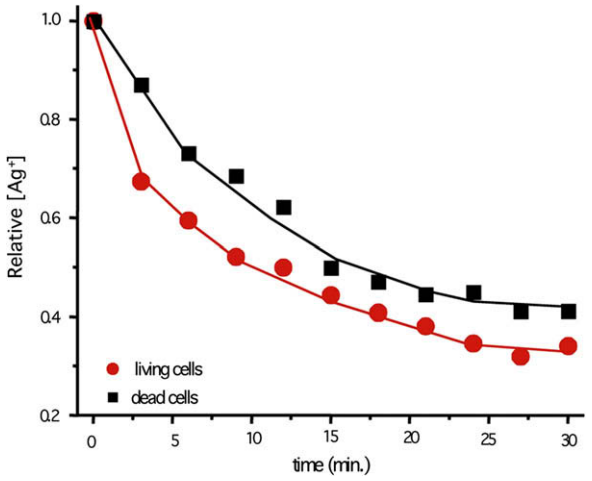

Fig. 7. The time-dependence of relative Ag^+ concentration in solution for living (red circles) and dead (black squares) HeLa cells in a culture medium containing 0.5 mM Ag+. HeLa cells are highly confluent with coverage of 90%. The lines are guides for the eye.

crease in the concentration of Ag^+ due to the adsorption of Ag^+ on the Petri dish.

The electrochemical results suggest that nearly 0.29 mM Ag^+ in solution was depleted by dead cells, attributable to complexation with inorganic functional groups on the cell surface or in the cytoplasm [50], with perhaps some reaction with residual formaldehyde. Living HeLa cells accumulated only about 10% more Ag^+ than the dead HeLa cells, suggesting that although 0.34 mM Ag^+ is depleted from the culture medium, most of the Ag^+ was bound to the outer surface of the plasma membrane without penetrating the membrane. The Ag^+ depletion difference is directly related to the uptake activity of living HeLa cells. Furthermore, as the two depletion curves of Ag^+ show nearly the same trends after 10 min (Fig. 7), Ag^+ depletion is most likely dominated by the adsorption process for both dead and living cells in this time region. On the other hand, HeLa cell viability plays a more important role for the first few min, which leads to the 10% difference between the dead and living HeLa cells.

5. Discussion

The electrochemical results suggest that HeLa cells can reduce $FcMeOH^+$. To achieve this activity, a HeLa cell needs to have an oxidoreductase system either within the cell or in the plasma membrane to transfer electrons across it. For example, a plasma membrane NADH-oxidoreductase (PMOR) system is able to transfer electrons from cytoplasm NADH inside the cell to extracellular electron acceptors, and it is located in the plasma membrane of all eukaryotic cells, including HeLa cells [51]. The PMOR system is necessary for maintaining the viability of mammalian cells in addition to the mitochondrial respiratory capacity [52]. The PMOR system, such as NADH-ferricyanide reductase, shows at least two distinct activities, an NADH-oxidase and a reductase, with a functional link between them. The rate of ferricyanide reduction by the NADH-ferricyanide reductase is ca. 20 pM/s/10^6 HeLa cells [50]. In our experiments, we did not observe any reduction of ferricyanide. However the estimated current for this reaction at a single HeLa cell scanned during a SECM experiment would be only 1.9 pA, which would be too small to detect as positive feedback compared to the oxidation current observed at the 10 μm Pt UME in solution containing 1 mM ferrocyanide. Thus, only negative feedback was observed from HeLa cells for ferrocyanide oxidation at the tip, as shown in Fig. 5C, because of the blocking effect of the cell. Simulation results, to be reported elsewhere, suggest that the effective heterogeneous rate constant for $FcMeOH^+$ reduction by the reductase of the HeLa cells is much faster than that of ferricyanide. As the standard potential for $FcMeOH^+$ reduction is more positive than that for ferricyanide, the NADH-ferricyanide reductase might exhibit a different rate towards $FcMeOH^+$ reduction. While the activity of each PMOR system is associated with different polypeptides, HeLa cells may contain an NADH-reductase that is active for $FcMeOH^+$ reduction. Both our experiments and previous reports suggest that the standard potential of the mediator is an important, but not sole, condition for reduction activity with HeLa cells. Another important factor, however, is the hydrophilicity of the mediator. HeLa cells generate positive feedback for the oxidation of hydrophobic mediators and negative feedback for the hydrophilic ones. Hydrophobic species are more likely to be able to diffuse into the plasma membrane and also into the cell, while hydrophilic species are excluded, except through special channels or pumps. Treatment of the cell with FcMeOH does not kill it, as measured by the near-identical positive feedback from the cell before and after long time exposure to a culture medium containing 1 mM FcMeOH. It also has a negligible effect on the cell viability as tested with Trypan blue.

Although large doses of silver ion may be toxic to mammalian cells and inhibit growth after long time exposure, no sign of apoptosis was observed. Fig. 6 indicates that Ag^+ in a culture medium with a concentration as high as 10 mM does not halt the activity of the HeLa cells over the short term. Previous electrochemical results [31] showed that 10 μm Ag^+ is lethal to bacteria such as *E. coli* with a concentration of 5×10^9 cell/mL, and the respiratory activity of *E. coli* ceased within 10 min. Thus, the tolerance concentration of HeLa cells to Ag^+ is more than 10^6 times that of *E. coli*. As the average mass and volume of a HeLa cell is only in the order of 10^3 times those of an *E. coli* cell, this high tolerance of the HeLa cell to Ag^+ strongly suggests that the HeLa cell and *E. coli* have different responses to Ag^+.

Living *E. coli* accumulated more than twice the amount of Ag^+ than dead ones based on electrochemical studies [31]. On the contrary, the concentration difference of Ag^+ depletion between the living and dead HeLa cells is only about 10%. This small difference suggests that most of the Ag^+ accumulates within the extracellular polysaccharide or on the cell wall [50], and only a small amount of Ag^+ can penetrate the membrane, interact with components in the cytoplasm, and stay inside the cell. Short-term silver toxicity studies of two freshwater algae suggest that silver toxicity is a direct result of intracellular accumulation, rather than cell surface interaction [28]. Thus, the relatively small difference of Ag^+ uptake by dead and living HeLa cells correlates well with the fact that HeLa cells are still active in a culture medium containing a high concentration of Ag^+.

6. Conclusions

SECM has proved to be a useful tool in probing the viability and activity of living cells. A living HeLa cell interacts with and reduces $FcMeOH^+$ and generates positive feedback to the tip current of FcMeOH oxidation during scanning. This positive feedback changes to negative when the HeLa cell is treated with a toxin, such as either CN^- or UVC. This change indicates that the feedback can be used to monitor the viability of HeLa cells on the bottom of a Petri dish. The feedback during SECM, positive or negative, with other mediators does not only depend upon their electrode potential, but is also related to the properties of the mediator like the hydrophobicity and charge.

As indicated by both O_2 reduction and FcMeOH oxidation, Ag^+ with a concentration as high as 10 mM has no detectable effect on the viability of HeLa cells over a time period of at least 1 h. This high resistance of HeLa cells towards Ag^+ correlates well with the small concentration difference for Ag^+ depletion between dead and living HeLa cells.

Acknowledgments

The support of this work by Nucryst Pharmaceuticals (Wakefield, MA) and the Robert A. Welch Foundation (F-0021) is gratefully acknowledged. We thank Dr. Lara K. Mahal and Lakshmipriya Krishnamoorthy (University of Texas at Austin) for generously providing HeLa cells for SECM experiments.

References

[1] M.A. Horton, P.P. Lehenkari, G.T. Charras, Roy. Soc. Chem. 283 (2002) 31–49 (Special publication).
[2] R.D. Schaller, C. Roth, D.H. Raulet, R.J. Saykally, J. Phys. Chem. B 104 (2000) 5217–5220.
[3] H. Minamitani, K. Tsukada, E. Sekizuka, C. Oshio, J. Pharmacol. Sci. 93 (2003) 227–233 (Tokyo, Japan).
[4] S.G. Megason, S.E. Fraser, Mech. Dev. 120 (2003) 1407–1420.

[5] B.R. Horrocks, G. Wittstock, in: A.J. Bard, M.V. Mirkin (Eds.), Scanning Electrochemical Microscopy, Marcel Dekker, NY, 2001, pp. 445–519.
[6] C. Cai, B. Liu, M.V. Mirkin, H.A. Frank, J.F. Rusling, Anal. Chem. 74 (2002) 114–119.
[7] M.A. Edward, S. Martin, A.L. Whitworth, J.V. Macpherson, P.R. Unwin, Physiol. Meas. 27 (2006) R63–108.
[8] B. Liu, W. Cheng, S.A. Rotenberg, M.V. Mirkin, J. Electroanal. Chem. 500 (2001) 590–597.
[9] B. Liu, S.A. Rotenberg, M.V. Mirkin, Anal. Chem. 74 (2002) 6340–6348.
[10] B. Liu, S.A. Rotenberg, M.V. Mirkin, Proc. Natl. Acad. Sci. USA 97 (2000) 9855–9860.
[11] T. Kaya, D. Numai, K. Nagamine, S. Aoyagi, H. Shiku, T. Matsue, Analyst 129 (2004) 529–534 (Cambridge, UK).
[12] M. Tsionsky, Z.G. Cardon, A.J. Bard, R.B. Jackson, Plant Physiol. 113 (1997) 895.
[13] R. Zhu, S.M. Macfie, Z. Ding, J. Exp. Bot. 56 (2005) 2831–2838.
[14] Y. Takii, K. Takoh, M. Nishizawa, T. Matsue, Electrochim. Acta 48 (2003) 3381–3385.
[15] W. Feng, S.A. Rotenberg, M.V. Mirkin, Anal. Chem. 75 (2003) 4148–4154.
[16] K. Takoh, A. Takahashi, T. Matsue, M. Nishizawa, Anal. Chim. Acta 522 (2004) 45–49.
[17] Y.-S. Torisawa, A. Takagi, H. Shiku, T. Yasukawa, T. Matsue, Oncol. Rep. 13 (2005) 1107–1112.
[18] J.M. Liebetrau, H.M. Miller, J.E. Baur, S.A. Takacs, V. Anupunpisit, P.A. Garris, D.O. Wipf, Anal. Chem. 75 (2003) 563–571.
[19] L. Pitta Bauermann, W. Schuhmann, A. Schulte, Phys. Chem. Chem. Phys. 6 (2004) 4003–4008.
[20] R.T. Kurulugama, D.O. Wipf, S.A. Takacs, S. Pongmayteegul, P.A. Garris, J.E. Baur, Anal. Chem. 77 (2005) 1111–1117.
[21] J. Mauzeroll, A.J. Bard, Proc. Natl. Acad. Sci. USA 101 (2004) 7862–7867.
[22] P.D. Bragg, D.J. Rainnie, Can. J. Microbiol. 20 (1974) 883–889.
[23] W. Ghandour, J.A. Hubbard, J. Deistung, M.N. Hughes, R.K. Poole, Appl. Microbiol. Biotechnol. 28 (1988) 559–565.
[24] W.J. Schreurs, H. Rosenberg, J. Bacteriol. 152 (1982) 7–13.
[25] P. Dibrov, J. Dzioba, K.K. Gosink, C.C. Hase, Antimicrob. Agents Chemother. 46 (2002) 2668–2670.
[26] L. Zeiri, B.V. Bronk, Y. Shabtai, J. Eichler, S. Efrima, Appl. Spectrosc. 58 (2004) 33–40.
[27] Q.L. Feng, J. Wu, G.Q. Chen, F.Z. Cui, T.N. Kim, J.O. Kim, J. Biomed. Mater. Res. 52 (2000) 662–668.
[28] D.-Y. Lee, C. Fortin, P.G.C. Campbell, Aquat. Toxicol. 75 (2005) 127–135.
[29] S. Franke, G. Grass, D.H. Nies, Microbiology 147 (2001) 965–972.
[30] S. Franke, G. Grass, C. Rensing, D.H. Nies, J. Bacteriol. 185 (2003) 3804–3812.
[31] K.B. Holt, A.J. Bard, Biochemistry 44 (2005) 13214–13223.
[32] J. Rungby, Dan. Med. Bull. 37 (1990) 442–449.
[33] A. Schedle, P. Samorapoompichit, X.H. Rausch-Fan, A. Franz, W. Fuereder, W.R. Sperr, W. Sperr, A. Ellinger, R. Slavicek, G. Boltz-Nitulescu, P. Valent, J. Dental Res. 74 (1995) 1513–1520.
[34] J.C. Wataha, C.T. Hanks, R.G. Craig, J. Biomed. Mater. Res. 28 (1994) 427–433.
[35] E. Hidalgo, C. Dominguez, Toxicol. Lett. 98 (1998) 169–179.
[36] A.J. Bard, M.V. Mirkin, Scanning Electrochemical Microscopy, Marcel Dekker, NY, 2001.
[37] J. Mauzeroll, E.A. Hueske, A.J. Bard, Anal. Chem. 75 (2003) 3880–3889.
[38] A.J. Bard, L.R. Faulkner, Electrochemical Methods, Wiley, NY, 2001. p. 458..
[39] M. Nishizawa, K. Takoh, T. Matsue, Langmuir 18 (2002) 3645–3649.
[40] T. Kaya, Y.-S. Torisawa, D. Oyamatsu, M. Nishizawa, T. Matsue, Biosens. Bioelectron. 18 (2003) 1379–1383.
[41] B. Liu, A.J. Bard, J. Phys. Chem. B 106 (2002) 12801–12806.
[42] M.P. Longinotti, H.R. Corti, Electrochem. Commun. 9 (2007) 1444–1450.
[43] A.P. Morocco, Crit. Care. Clin. 21 (2005) 691–705.
[44] N.A. Cridland, M.C. Martin, K. Stevens, C.A. Baller, A.J. Pearson, C.M.H. Driscoll, R.D. Saunders, Int. J. Radiat. Biol. 77 (2001) 365–374.
[45] D. Bettega, P. Calzolari, F. Belloni, F. Di Lena, S. Genchi, M. Lupi, P. Massariello, S. Orsini, L. Tallone, D. Tomasoni, P. Ubezio, J.L. Redpath, Int. J. Radiat. Biol. 77 (2001) 963–970.
[46] M.H. Wu, J.H. Chang, C.C. Chou, B.Y.M. Yung, Int. J. Cancer 97 (2002) 297–305.
[47] L.F. Barros, Pfluegers Arch. 437 (1999) 763–770.
[48] L.J. Reitzer, B.M. Wice, D. Kennell, J. Biol. Chem. 254 (1979) 2669–2676.
[49] J. Orczyk, D.M. Morre, D.J. Morre, Mol. Cell. Biochem. 273 (2005) 161–167.
[50] M.L. Merroun, N.B. Omar, E. Alonso, J.M. Arias, M.T. Gonzalez-Munoz, Geomicrobiol, J. 18 (2001) 183–192.
[51] D.J. Morre, Methods Enzymol. 378 (2004) 179–199.
[52] J.A. Larm, E.J. Wolvetang, F. Vaillant, R.D. Martinus, A. Lawen, A.W. Linnane, Protoplasma 184 (1995) 173–180.